Knocking out the Language-Associated Gene

Verifying the efficacy of CRISPR-Cas9-directed cleavage of bat and human DNA to aid the development of a *FoxP2* knockout *Phyllostomus discolor* animal model

Erika Blažková

Supervised by Prof. Sonja C. Vernes
Principal Investigator of the Neurogenetics of Vocal Communication Research Group

School of Biology

Funded by Lord Laidlaw and the Laidlaw Foundation

Abstract

FOXP2 is crucial for neurodevelopment in humans. Altered FOXP2 expression in cells has been found to affect language and speech development. In recent years, bats such as *Phyllostomus discolor* are emerging as models for the study of the neurogenetics of vocal communication. We seek to develop a *FoxP2* knockout bat to shed light on biological and evolutionary mechanisms of FoxP2 in vocal production learning. This study aimed to verify the efficacy of chosen guide RNA to lead Cas9 to cleave in the correct position in the *FoxP2*/*FOXP2* sequence in bat and human DNA. Chosen guides successfully drove Cas9 cleavage in the correct positions in both species' DNA. The success of this protocol provides support for further study in vitro, hopefully leading to the successful execution of a CRISPR-Cas9-directed knockout of bat *FoxP2* in vivo.

1 BACKGROUND

FOXP2 and vocal learning

Vocal production learning refers to learning sounds and modifying vocalisations in accordance with experiences with vocalisation of other individuals (Janik and Knörnschild 2021). Vocal learning has been observed in seals, elephants, whales, and some species of ape, bird, and bat (Vernes et al. 2022). The association of the FOXP2 protein with vocal learning in humans was famously observed by Dr. Lai at the University of Oxford in 2001 (Lai et al 2001).

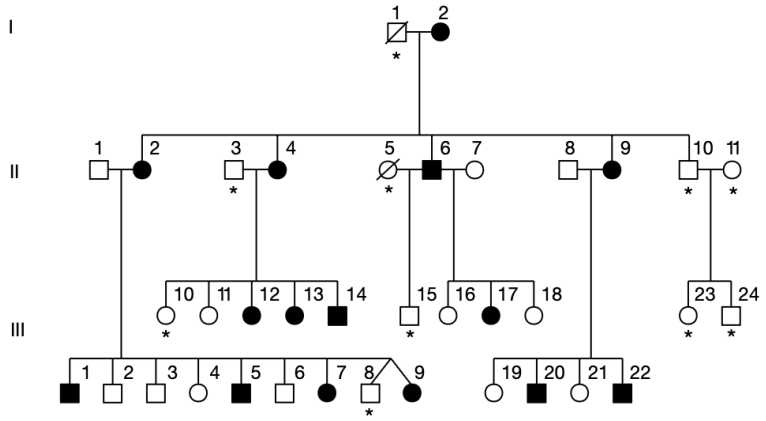

Fig 1: pedigree of KE family. Squares represent males, circles represent females. Shading denotes individuals who carry the monoallelic autosomal dominant R533H mutation in the *FOXP2* gene. Diagonal lines denote deceased individuals. Asterisks denote individuals who were unable for linkage analysis (figure from Lai et al, 2001).

The affected members of the KE family (see figure 1) presented with a lack of coordination of orofacial muscles, a limited vocabulary and difficulties with speech comprehension (MacDermot et al. 2005, Feuk et al. 2006, Reuter et al. 2017). The KE family carried a monoallelic autosomal dominant point mutation in the forkhead box region of *FOXP2*, which codes for the DNA binding region of FOXP2 (Lai et al 2001). An altered sequence often leads to loss of function because the sequence's transcribed mRNA strands are identified as faulty by the cell and digested via nonsense-mediated decay (wherein the faulty strand in tagged with ubiquitin, which is then identified and bound to by a digestion enzyme). However, FOXP2 is a transcription factor, and its function hinges on its ability to bind to DNA, hence a mutation in its DNA-binding region silences its expression whether the cell tags its transcriptions with ubiquitin or not. Since Lai's original report, focus on FOXP2's molecular mechanisms have revealed a multitude of downstream effects key for neurodevelopment and signalling, including neuronal migration, neuronal connectivity, microtubule dynamics, and pre-/post-synaptic inhibitory and excitatory currents (den Hoed et al. 2021).

FOXP2's significance in vocal production learning lends itself to the importance of making use of in vivo models to investigate FOXP2's function across the gene–behaviour axis (Gorden, Amini and White 2013). Currently, the most commonly utilised mammalian model for *Foxp2* manipulation is *Mus musculus* (mice), while FOXP2's role in vocal production learning is most commonly modelled on *Taeniopygia castanotis* (zebra finches). *Foxp2* knockout mice have shown decreased neurite outgrowth, altered GABA-mediated (Gamma-aminobutyric acid: an inhibitory neurotransmitter) inhibition and excitation, decreased motor learning ability, and some altered context-dependent vocalisation. (French et al. 2012, Fujita et al. 2008, Druart 2020, Chen et al. 2016, van Rhijn et al. 2018, Ahmed et al. 2024). *FoxP2* knockout zebra finches likewise exhibit decreased neurite outgrowth, and have additionally shown decreased birdsong learning ability, altered inhibitory and excitatory signalling in dopaminergic pathways (which are involved in birdsong production in zebra finches), and significantly altered context-dependence vocalisation. (Haesler et al. 2007, Burkett et al. 2018a, Murugan et al. 2013, Schultz et al. 2010).

Bats, like humans, are both mammals and vocal production learners. Studying the mechanisms of FoxP2 in bats and comparing results with findings from other animal models, and from human patients, may hence provide unique and valuable insight into FoxP2 and its downstream effects.

FoxP2 knockout in *Phyllostomus discolor*

Attempts to generate a *Phyllostomus discolor (P. discolor)* knockout of *FoxP2*, though commonly showing promise in vitro, have thus far been unsuccessful in inducing a knockout in vivo. (J. Mengede 2021, unpublished data; Groot 2026). Initial attempts to knockdown FoxP2 expression with RNAi did not significantly change intracellular FoxP2 levels. (J. Mengede 2021, unpublished data; Groot 2026). Attempts to induce nonsense-mediated decay of *FoxP2* translations by CRISPR-SaCas9 (Groot 2026) equally did not significantly lower FoxP2 expression in vivo.

FOXP2 is one of four genes in the FOXP family, which is in turn part of the wider FOX family – "FOX" referring to the forkhead box, which is widely conserved in FOX genes. (Weigel & Jackle 1990, Hannenhalli & Kaestner 2009). FOXP genes typically contain a Q-rich region, the leucine zipper and zinc finger, and the forkhead box coding for the DNA binding domain. (Wang et al. 2003).

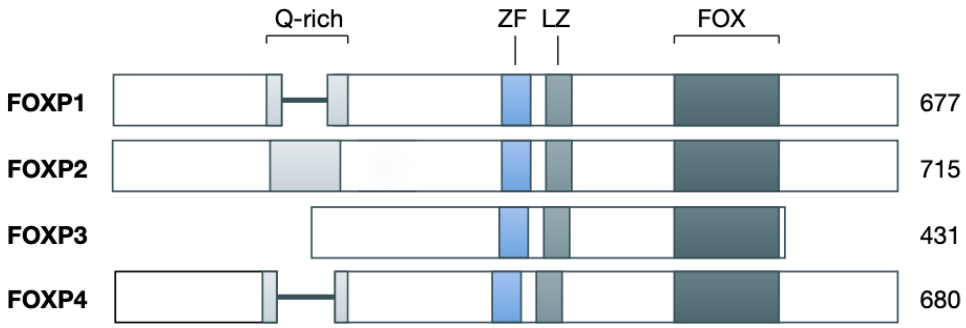

Fig 2: The structure of FOXP family genes (figure from den Hoed et al. 2021). The leucine zipper (LZ), zinc finger (ZF) and forkhead box (FOX) are highly conserved in all four genes, and the Q-rich region appears in all genes but *FOXP3*. Of the four, *FOXP3* diverts most in terms of its structure and function. *FOXP1*, *FOXP2*, and *FOXP4* are over 90 % homologous in structure.

FOXP proteins have a highly conserved structure, with FOXP1, FOXP2, and FOXP4 being over 90 % homologous at the amino acid level. The highest degree of conservation is in the forkhead box region. (Weigel & Jackle 1990; Hannenhalli & Kaestner 2009).

FoxP2 is a transcription factor, and any mutation induced in its forkhead box region, which codes for the DNA binding domain of the FoxP2 protein, would silence the expression of its translations, without needing to rely on nonsense-mediated decay (den Hoed et al. 2021).While targeting the forkhead box

would present a greater risk of Cas9 being guided to bind to a forkhead box sight on a different *FOXP* gene (referred to as 'offsite binding'), the lack of success experienced when relying on nonsense-mediated decay instead suggests it as a possible solution.

Phyllostomus discolor

Bats have been identified as potential mammalian models of vocal production learning. Notably, vocal production learning has been observed in juvenile Egyptian fruit bats (*Rousettus aegyptiacus*), juvenile male sac-winged bats (*Saccopteryx billineata*), greater spear-nosed bats (*Phyllostomus hastatus*), and pale spear-nosed bats (*Phyllostomus discolor*) (Taub, Prat and Yovel 2014, Knörnschild et al. 2010, Boughman 1998, Vernes et al. 2022). In particular, isolation calls (used in parent-offspring identification) of hand-reared juvenile pale spear-nosed bats were found to undergo adjustment per external acoustic reference provided by a computer playback in the absence of conspecific vocalisations (Esser 1994), and vocalisation patterns of *P. discolor* individuals deafened from an early age showed similar patterns as observed in deaf children, including a lower range of receptive vocabulary (Merchan et al. 2022). Further, pale spear-nosed bats have been observed to be able to modify the contents of their social calls in adulthood, providing evidence for the persistence of vocal production learning throughout their lifetimes. (Lattenkamp et al. 2018, 2020)

Beyond vocal production learning and possession of mammalian brain structures, *P. discolor* gregarious nature and capacity to thrive in captive colonies make them appropriate candidates for the study of the neurogenetic underpinnings of vocal learning. (Vernes et al. 2022).

A viable *FoxP2* knockout of a mammalian vocal production learner would allow comparison with other mammals and vocal learners to shed light on biological and evolutionary mechanisms governing the role of FoxP2 in vocal production learning, with potential applications in human education and healthcare.

Aims

Our aim is to aid the knockout of *FoxP2* in *Phyllostomus discolor* in hopes of generating a transgenic model that could be studied to aid understanding of the gene–morphology–behaviour integration of FoxP2's function.

2 METHODOLOGY

2.1 TECHNOLOGIES

We performed a DNA digest analysis of Cas9 cleavage (see figure 3) of *FoxP2* in PCR amplicons (see figure 4) of DNA taken from two bat individuals (Doris and an unnamed Dead Juvenile (DJ)), and of *FOXP2* in PCR amplicons of DNA taken from human embryonic kidney (HEK) cells.

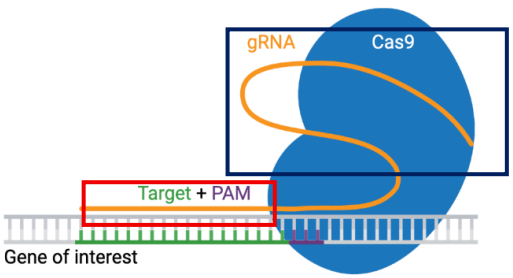

Fig 3: Cas9 is guided to a gene of interest by guide RNA. (figure from "Addgene: CRISPR Guide." 2014).The

conserved part of guide RNA (dark blue/black box) binds to Cas9, while its variable section (red box) is an antisense strand compatible with the gene of interest. Cas9 cleaves three base pairs upstream from the Protospacer Adjacent Motif (PAM). Sitting downstream from the gene of interest, PAM is a short, conserved sequence crucial, in archaea and bacteria, for identifying non-self DNA.

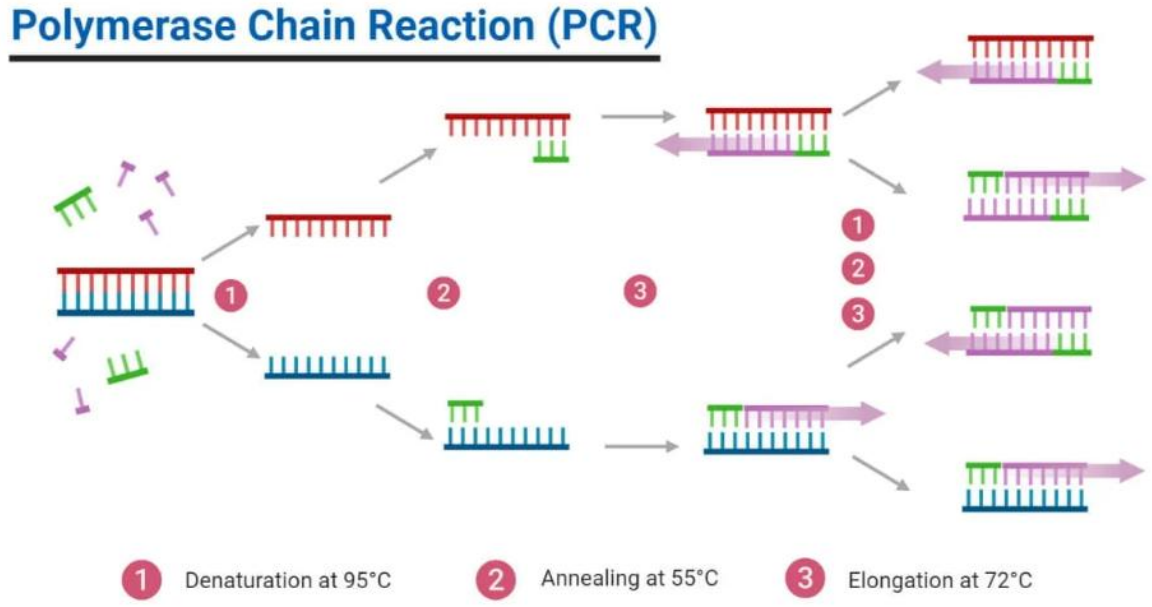

Fig 4: (figure from https://microbenotes.com/pcr-principle-enzymes-steps-types-uses/, Dahal 2025). PCR amplification is semi-conservative. Additional copies of DNA are created by separating the parent strands of double-stranded DNA and making up the antisense strand to each of them, using the parent as a template. Hence, one DNA double-helix is split into two, each represented by one parent strand. In this way, every consecutive cycle results in the doubling of the total number of DNA copies.

Guide RNA has been chosen from the guides designed as part of the original CRISPR-Cas9 study (figure 5, from Groot 2026). The guides chosen (guide 7 and guide 8) sit near or in the forkhead box to enable cleavage in this region. When choosing guides, the factors that ensure a successful knockout must be considered. The success of CRISPR-Cas9-driven gene knockout relies on three processes (Suresh 2021, Groot 2026). First, successful cleavage at the correct position by the Cas9 complex. Second, the employment of non-homologous end joining as a repair pathway by the cell, meaning that the break is repaired by the insertion of random nucleotides, thereby altering the sequence. Third, nonsense mediated decay – the removal of gene transcriptions identified as faulty. If a break is induced in a key region whose alteration is inherently fatal to the protein's function, nonsense mediated decay is not necessary.

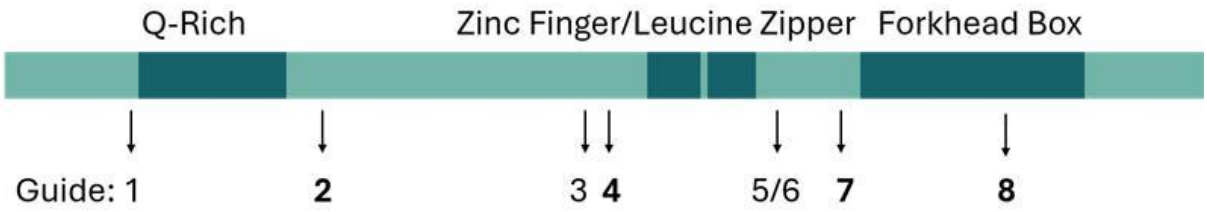

Fig 5: Diagram of *FoxP2*, including denotation of Q-rich, zinc finger, leucine zipper, and forkhead box areas, showing where different guide RNA would lead Cas9 to cleave. (Figure from Groot 2026.)

Guides are chosen based on their distance from the C- and N-terminuses, their efficiency, whether the position they sit at is highly conserved in a family of genes, and whether the area they target is a match to the human equivalent (Groot 2026). Of the guides shown in figure 5, guides 3, 5, and 6 were not a

match when compared against the human gene (Groot 2026). Guide 1 showed a lack of activity upon further testing. Though guides 2 and 4 showed promise in vitro, they did not succeed in vivo. Guides 7 and 8 were initially dismissed for their proximity to both the C-terminus and the forkhead box, which is highly conserved in FOXP proteins and poses a risk of offsite binding. They were revisited after the failure of guides 2 and 4. While there is a greater risk of offsite binding, they have potential to induce a mutation in the forkhead box region, which, if successful, would eliminate dependence of knockout on nonsense-mediated decay. Hence, guides 7 and 8 were chosen for this study.

A primer optimisation step was included before PCR amplification to test each primer pairs' specificity (i.e.: their ability to amplify one specific region, and no other), and to identify the temperature at which respective primer pairs would be most effective in promoting amplification.

Both chosen bat DNA samples will be run against experimental guides 7 and 8. Human embryonic kidney DNA samples will be run against experimental guides 7 and 8, and against positive control guide 4.

2.2 PROCEDURE

Primer Optimisation

Given the small size of the area being worked with (around 500 base pairs), the importance of a given starting fragment size for gel electrophoresis analysis of fragmentation after the DNA digest, and the importance of a large volume of DNA for gel imaging, primers must be optimised for specificity and strength of amplification. Primer pairs are tested by running them at a series of different temperatures (see Appendix 1) in a PCR machine with the same components that the actual PCR amplification is then run with. Specificity is determined by the presence of a single band as opposed to multiple bands. Strength is determined by band intensity. The more specific primer pairs are chosen over less specific primer pairs. For the primer pairs chosen, the temperature at which amplification is the strongest is the one at which PCR amplification is run. Different primer pairs may have different optimal temperatures.

Primer specificity was tested by running them through a PCR amplification cycle. Two primer pairs per guide were tested in each species. Each primer pair was tested using a temperature gradient to identify the temperature at which the strength of amplification was greatest (see Appendix 1, Table 2).

A PCR Master Mix of 90uL containing Q5 High-Fidelity 2X Master Mix, template DNA, and nuclease-free water was prepared for each of the two species. As there were two primer pairs being tested per species, forward and reverse primers were added later. Volumes of each component were added per manufacturer's instructions.

A 2% Agarose Gel with SybrSafe was prepared. After PCR, 1ul of 6x Orange G was added to 5uL of the PCR-amplified samples. 2ul of Ladder (Generuler 100bp plus) was used. The gel was run at 100V for approximately 35 minutes and imaged in UviDoc.

For each guide, a primer pair that had exhibited high specificity was selected.

PCR amplification

PCR amplification is necessary to increase the volume of DNA available and thus enable analysis by Gel electrophoresis; if the volume of DNA is too low, bands denoting differently sized fragments with not show up upon gel imaging or will be very weak. PCR amplification is, through the use of primer pairs, also used to amplify the area of HEK and bat DNA that is relevant to the study. Working with large strands of DNA is more burdensome and inefficient than working with smaller strands. Primer pairs provide anchor-points between which the components of the Q5 Master Mix can act to amplify DNA.

Product sizes for PCR amplification were calculated on Benchling (see Appendix 1, Table 3). PCR amplification was performed using the previously identified optimal annealing temperature. 200ng of template DNA as measured by nanodrop was used. Two PCR amplifications were performed for each of the sample DNA: one with the optimal species-specific guide 7 primer pair, one with the optimal species-specific guide 8 primer pair. The final volume of each PCR amplification component was 50uL. Nuclease-free water volume was adjusted with regards to the volume of DNA added. Volumes were added per manufacturer's instructions.

After PCR, 4uL of the PCR amplified samples were run on a 2% agarose gel (100ml TAE, 2g agarose, 10uL SybrSafe, 0.8uL Orange G per sample, 2uL of 100bp NEB ladder) to confirm accurate amplification.

Gel electrophoresis is used for separation of differently sized fragments of DNA. DNA fragments are negatively charged due to their phosphate backbone and run from the negative to the positive charge through an agarose gel. The agarose gel provides resistance, hence smaller fragments with a smaller surface area travel faster and lower than larger fragments over the same period of time. In this study, gel electrophoresis is used to a.) verify the specificity of primers used in PCR amplification, b.) determine the temperature at which the strength of amplification is the greatest for different primer pairs, c.) verify that amplification had occurred, and d.) check for Cas9 cleavage efficiency post-DNA digest.

The gel ran for 35 minutes at 100V. While the gel ran, the remaining sample volumes were measured and underwent PCR cleanup.

PCR cleanup

PCR cleanup is performed post-PCR amplification to isolate DNA amplicons away from unwanted particles that could contaminate the DNA digest. Isolated DNA is resuspended in a chosen buffer, its concentration is checked on a Nanodrop, and samples are diluted according to their starting concentrations to a common concentration – in our case 30nM.

PCR Cleanup was performed using the Monarch NEB PCR Cleanup Kit, following the manufacturer's protocol with minor modifications: (1) Prior to elution, columns were spun in a clean collection tube for 1 minute to dry the filter membrane, and (2) elution was performed in 2x spins of 6ul of gently warmed (37C) elution buffer incubated for 1-5 minutes each time.

After PCR cleanup, sample concentrations were measured on nanodrop. Samples were then diluted to 30nM.

DNA digest

A DNA digest was performed to verify the ability of guide RNA to guide Cas9 to cleave in the correct position in chosen DNA samples. The DNA digest solution was made up of NEBuffer 3.1, Cas9, guide RNA (aka guide RNA), and the post-PCR amplification, post-PCR cleanup DNA sample. Each condition (DJ DNA guide 7, DJ DNA guide 8, Doris DNA guide 7, Doris DNA guide 8, HEK DNA guide 7, HEK DNA guide 8, and HEK DNA guide 4) was run once with Cas9 and guide RNA, and once with Cas9 but without guide RNA. This was to ensure that additional bands on the gel were caused by guide-directed Cas9 cleavage, and not by contamination.

All recommendations given by the manufacturer for the proper storage and use of substances were followed.

A 300nM guide RNA sample was prepared by diluting the 10uM stock with nuclease-free water on ice. A 1uM Cas9 sample was prepared by diluting the 20uM stock in NEBuffer 3.1. The reaction was prepared per the volumes below. The volumes below are volumes for 1 reaction:

Table 2: volumes for one DNA digest reaction

COMPONENT	**Amount / Rx (High Concentration Version)**
Nuclease-free water	**13ul**
NEBuffer 3.1	**3ul**
300 nM guide RNA *(or H2O for Cas9 only condition)*	**6ul**
"1 µM Cas9 Nuclease, S.pyogenes (M0386S)"	**2ul**
Reaction volume	**24ul**

A Master Mix of nuclease-free water, NEBuffer 3.1, and SaCas9 nuclease was prepared, with volumes multiplied by the number of reactions being run plus two. 12 reactions were run in the initial DNA digest. For each guide in each DNA sample type a Cas9+guide RNA and a Cas9 only condition were run to ensure that bands observed in the successive gel were not caused by contamination of any of the components.

All PCR amplicons were incubated either with or without the relevant guide.

Samples were pre-incubated for 10 minutes at 25 °C. 6 µL of a 30 nM of the relevant substrate DNA was added to each reaction. The mixture was mixed thoroughly and pulse-spun in a microfuge, then incubated at 37 °C for 30 minutes. 2µL of Proteinase K was then added to each sample. The mixture was mixed and pulse-spun in a microfuge, then incubated at 37 °C for 15 minutes.

Samples were run on a 2.5% SybrSafe-stained agarose gel for 30 minutes at 70V, with 2.5µL of Orange G ladder on either side.

Gels were visualised on UviDoc.

% gene editing was calculated per the following equation:

$$\%\ editing = 100 \times (1 - \sqrt{1 - \frac{(\sum band\ intensity_n) - band\ intensity_1}{\sum band\ intensity_n}}$$

3 RESULTS

3.1 PRIMER OPTIMISATION

Optimal temperatures for chosen primers were determined as between 62 and 66 degrees Celsius. The temperature gradient for PCR amplification was set accordingly.

Table 1: Primer pairs and temperatures chosen per their specificity and strength. PCR amplification product length calculated per library values on Benchling.

Primer Name	Sequence of primer pair	Product Length	Q5 Annealing Temp
G7Fwd1 Human	GGGGCAGTCGATAATCAGCA	599	**66** degrees Celsius
G7Rev1 Human	TGCTCTGGAATGGCTCATGT	(incl. Forward and Reverse)	66 degrees Celsius
G8Fwd2 Human	CAGGGACACAACAGAGCTGA	588	**66** degrees Celsius
G8Rev2 Human	TGCAGTTCATTGCCACGAGA	(incl. Forward and Reverse)	66 degrees Celsius
G7Fwd2 Bat	ACCTCTACCAGCAGCCTCTA	500	**65** degrees Celsius
G7Rev2 Bat	GACTCCAGTTTCCATGTGCTC	(incl. Forward and Reverse)	65 degrees Celsius
G8Fwd2 Bat	TGTTTGGCTGCCTTATTAAGCA	501	**62** degrees Celsius
G8Rev2 Bat	TGCATGAAAACAGGCAGGTG	(incl. Forward and Reverse)	62 degrees Celsius

3.2 DNA DIGEST GEL ELECTROPHORESIS

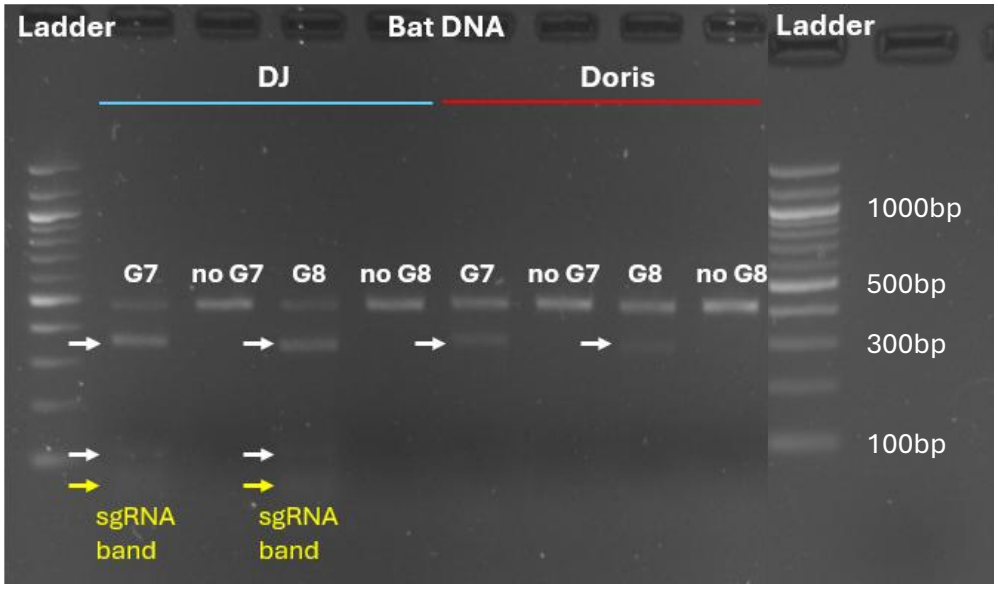

Fig 6: DNA digest bat DNA. White arrows denote (visible) DNA fragments. Yellow arrows denote (visible) bands that are caused by the migration of guide RNA.

Bat wing punch DNA samples containing both guide RNA and Cas9 separated into multiple bands, as expected when the sample DNA has undergone fragmentation, while samples containing only Cas9 without guide RNA remained as a singular band (see comparison between lane 'G7' and lane 'no G7'). Fragments gained appear to have been of an appropriate size per predicted values (just under 500 base pairs for unfragmented bands, and under 400 and around 100 base pairs for fragmented bands). The size of fragments corresponding to predicted values verified that cleavage was occurring at the correct position.

DNA digest demonstrated digestion of bat wing punch DNA in both guide 7 and guide 8 conditions, and not the guideless (Cas9-only) control. Subsequently, PCR amplification and DNA digest of HEK DNA guide 7 and 8 was replicated and run against a previously validated positive control guide 4.

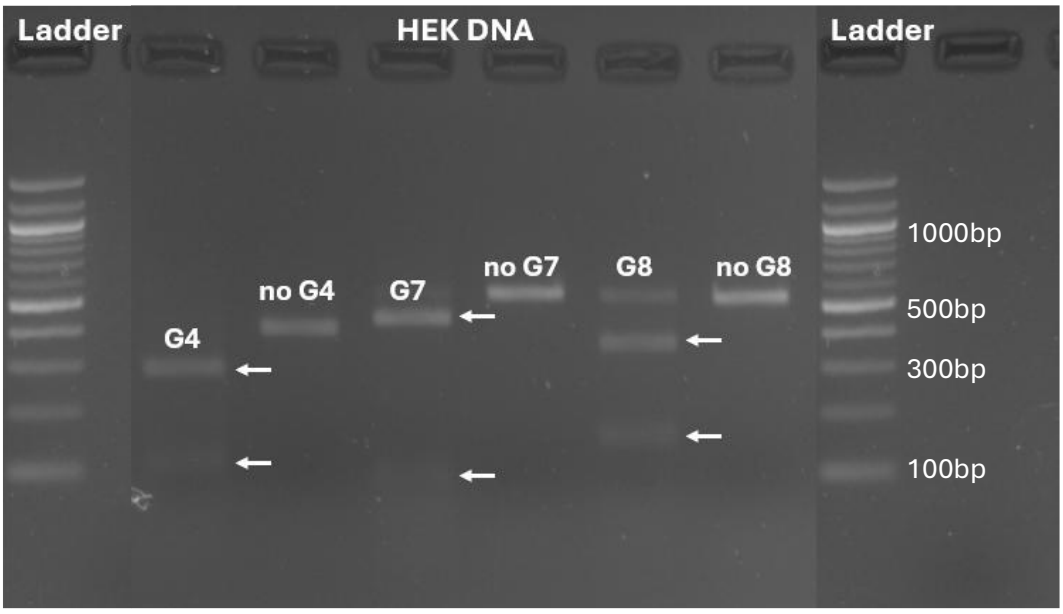

Fig 7: DNA digest HEK DNA. White arrows denote (visible) DNA fragments. All samples that contained guide RNA underwent cleavage and separated into fragments.

HEK DNA samples containing both guide RNA and Cas9 separated into multiple bands, as expected when the sample DNA has undergone fragmentation, while samples containing only Cas9 without guide RNA remained as a singular band (see comparison between lane 'G7' and lane 'no G7'). Fragments gained appear to have been of an appropriate size per predicted values. Unlike with bat wing punch DNA, these varied significantly between conditions. The size of fragments corresponding to predicted values verified that cleavage was occurring at the correct position. The positive control guide 4 condition showed large cleavage efficiency, with the unfragmented band being barely visible in the guide RNA + Cas9 condition, even when the image of the gel underwent overexposure. Guide 4 has been shown to drive cleavage efficiently in HEK DNA in past replications. The success of the guide 4 positive control bodes well for the integrity of the procedure.

Gel analysis of the replicated DNA digest found guide 7 and guide 8 cleavage of HEK DNA. Positive control guide 4 cleavage in HEK DNA was successfully replicated.

3.3 Analysis

Highest cleavage efficiency was in guide 4 in HEK DNA. High cleavage efficiency was shown by HEK DNA in the guide 7 and 8 conditions likewise. In Bat DNA, while wing clipping DNA taken from DJ showed high cleavage efficiency in both guide 7 and guide 8, DNA taken from Doris showed significantly less cleavage efficiency than both HEK DNA and DJ DNA.

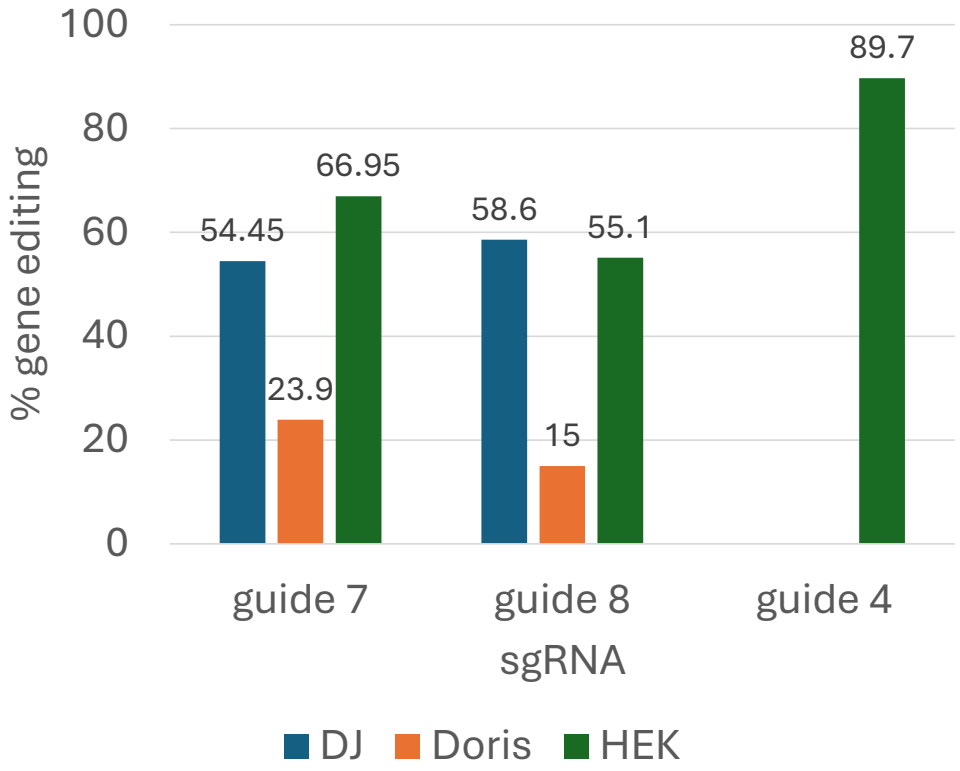

Fig 8: Graph showing differences in mean cleavage efficiency per guide per species/individual.

4 DISCUSSION

Gel analysis found cleavage in all tested guides in HEK and DJ DNA. Much like with guide RNA used in prior CRISPR-Cas9 knockout generation attempts, guides 7 and 8 were met with success in DNA. Fragments sizes agreed with predictions, indicating that guides are driving Cas9 cleavage in the expected area. There was relatively low cleavage efficiency found in Doris wing punch DNA as opposed to DJ wing punch DNA. This may be explained by high sensitivity of DNA digest analysis to small differences in DNA digest solution proportions. This high sensitivity was suggested in the change of calculated DJ DNA cleavage efficiency, where the difference between calculated percentage efficiencies in gels 1 and 2 was above 10 percent (10.7 %, see Appendix 4). Differences in Cas9 cleavage efficiency in DJ and Doris may also have been partially caused by intraspecies variation between DJ and Doris's genomes, or by pipetting error. Pipettes, like all measuring tools, have a margin of error, so pipetting error leading to small differences in DNA digest solution proportions may be the most likely explanation.

In all conditions excepting guide 8, where cleavage in bat DNA showed higher efficiency than that in HEK DNA, human embryonic kidney DNA exhibited more efficient Cas9 cleavage than bat DNA. Further, there was variation observed in Cas9 cleavage in different bat individuals. This suggests that further optimisation may be necessary to ensure the dependability of *FoxP2* knockout in different bat individuals.

Importantly, the DNA digest showed that experimental guides 7 and 8 drive cleavage of both human and bat FOXP2 DNA.

Having verified their ability to guide Cas9 to cleave in the correct spot, further testing must be conducted to verify that Cas9 cleavage is leading to an altered sequence. Cleavage results in an altered sequence when the cell employs non-homologous-end-joining (NHEJ) – wherein arbitrary nucleotides are drafted from the intracellular matrix and inserted between the two separated ends – to repair the break. NHEJ activity will be verified by T7E1 analysis in human (HEK293) cells. The T7E1 endonuclease checks for nonhomology in DNA, which is what the insertion of arbitrary nucleotides during NHEJ would result in. Once NHEJ activity is verified, testing in bat cells and individuals may proceed.

Future research and implications

For our purposes of developing a viable *FoxP2* knockout *P. discolor* vocal learning model, the most important thing is to proceed to T7E1 analysis in cell culture to verify the employment of the NHEJ repair pathway after cleavage. The Cas9 protein is being guided to the forkhead box region of *FOXP2*. The forkhead box region codes for the DNA binding domain of FOXP2. Because FOXP2 is a transcription factor, any alteration in this region should prove fatal to its function. While cells undergoing mitosis have been observed to employ a repair pathway that results in no alterations in the sequence (homology-directed repair), neuronal cells, which we are targeting, are non-mitotic, and should hence be employing only the NHEJ repair pathway.

A challenge that may arise in attempting to apply Cas9-directed cleavage in vivo is offsite binding (Groot 2026). The forkhead box, apart from coding for the DNA binding domain, is also highly conserved between *FOXP* genes (Weigel and Jackle 2009). The similarity is most stark between *FOXP2* and *FOXP1*, and, to a lesser degree, *FOXP4*. In an in vivo scenario, this may result in the chosen guides accidently guiding Cas9 to bind to *FOXP1* instead of *FOXP2*, potentially knocking out the wrong gene. This can fortunately be tested for after application by measuring levels of expression of other FOXP proteins alongside FOXP2.

Turning in vitro success into in vivo application is notoriously tricky. In an investigation into data from 2022, the IQVIA institute found that only about seven percent of drugs in drug development maintained efficacy beyond the in vitro–in vivo transition (Aitken et al. 2023).

In vitro efficacy is crucial in determining a technique's viability for application (Patel and Patel 2024). However, an in vivo environment is significantly more changeable and heterogenous, and significantly less subject to experimental control, than a cell assay or DNA sample (Liu et al. 2025). Actors that otherwise demonstrate good coordination with one another in a well-controlled in vitro environment may present as less efficient or fully unviable in vivo. While more complex in vitro models – such as organoids – have been developed, some with heterogeneity that mimics sections of in vivo tissue, they remain costly and difficult to upkeep (Li et al. 2024). Additionally, their complexity reduces the level of possible experimental control. Reduced control and increased heterogeneity between samples lowers replicability between trials. Hence, simpler models are needed to verify the viability of a method through the reliable replication of results.

FOXP2 is a developmentally significant transcription factor involved in reaction cascades throughout the body (den Hoed et al. 2021), and its in vivo study is crucial in building the foundation needed for the development of therapies targeting disorders caused by alterations in its expression or by the activity of a protein included in its downstream effects. So far, in vivo FoxP2 knockouts have only been generated in a handful of species, including *Mus musculus*, *Taeniopygia castanotis*, and *Drosophila* (Fujita-Jimbo et al. 2026). Valuable insights have been gained from these models, including into FoxP2's role in context-dependent vocalisation, motor learning, and neurite outgrowth. Animal models have further implicated FoxP2 in prenatal development, cell proliferation, morphogenesis and immunity, and studies investigating the effect of the up and down regulation of its expression have found it capable of modulating the progression of complex conditions like chronic kidney disease (Zou et al. 2025), prostate cancer (Zhu et al. 2023), Huntington's disease (Hachigian et al. 2017), speech-language disorder, and autism spectrum disorder (Fujita-Jimbo et al. 2026). Study of FoxP2 activity in different species – especially in mammals and vocal production learners – could help strengthen our understanding of its evolutionary and biological mechanisms enough to be able to reckon with these more complex pathologies.

While gene therapy is still an emerging field, the year 2023 saw the approval of two gene therapy products for sickle cell disease (SCD), a family of inherited red blood cell (RBC) disorders where RBCs are crescent- instead of disc-shaped, affecting oxygenation and blood flow (Sharma et al. 2026). Both therapies lead to persisting desired disease modification with acceptable short-term toxicity.

This and similar successes demonstrate the potential of gene-protein research application in healthcare. Continued study of the genetic and molecular mechanisms of FOXP2 may enable healthcare systems to develop better treatment methods for conditions where its activity is implicated, including for speech apraxia of the kind observed in the KE family in 2001.

5 REFERENCES

Addgene. n.d. 'Addgene: CRISPR Guide'. Accessed 18 August 2026. https://www.addgene.org/guides/crispr/.

Ahmed, Newaz I., Nitin Khandelwal, Ashley G. Anderson, Ashwinikumar Kulkarni, Jay R. Gibson, and Genevieve Konopka. 2024. 'Compensation between FOXP Transcription Factors Maintains Proper Striatal Function: Cell Reports'. Cell Press journal. https://doi.org/10.1016/j.celrep.2024.114257.

Aitken, Murray, Nicole Connelly, Michael Kleinrock, and Jamie Pritchett. 2024. '(PDF) Global Trends in R&D 2023'. IQVIA. https://www.researchgate.net/publication/388070887_Global_Trends_in_RD_2023.

Boughman, J. W. 1998. ‘Vocal Learning by Greater Spear-Nosed Bats’. Proceedings. Biological Sciences 265 (1392): 227–33. https://doi.org/10.1098/rspb.1998.0286.

Burkett, Zachary Daniel, Nancy F. Day, Todd Haswell Kimball, et al. 2018. ‘FoxP2 Isoforms Delineate Spatiotemporal Transcriptional Networks for Vocal Learning in the Zebra Finch’. eLife Sciences Publications, Ltd. https://doi.org/10.7554/eLife.30649.

Chen, Yi-Chuan, Hsiao-Ying Kuo, Ulrich Bornschein, et al. 2016. ‘Foxp2 Controls Synaptic Wiring of Corticostriatal Circuits and Vocal Communication by Opposing Mef2c’. Nature Neuroscience 19 (11): 1513–22. https://doi.org/10.1038/nn.4380.

Dahal, Prashant. 2025. Polymerase Chain Reaction (PCR): Principle, Enzymes, Steps, Types, Uses. Biochemistry. August 11. https://microbenotes.com/pcr-principle-enzymes-steps-types-uses/.

Druart, Mélanie, Matthias Groszer, and Corentin Le Magueresse. 2020. ‘An Etiological Foxp2 Mutation Impairs Neuronal Gain in Layer VI Cortico-Thalamic Cells through Increased GABAB/GIRK Signaling’. Research Articles. Journal of Neuroscience 40 (44): 8543–55. https://doi.org/10.1523/JNEUROSCI.2615-19.2020.

Esser, K. H. 1994. ‘Audio-Vocal Learning in a Non-Human Mammal: The Lesser Spear-Nosed Bat Phyllostomus Discolor’. Neuroreport 5 (14): 1718–20. https://doi.org/10.1097/00001756-199409080-00007.

Feuk, Lars, Aino Kalervo, Marita Lipsanen-Nyman, et al. 2006. ‘Absence of a Paternally Inherited FOXP2 Gene in Developmental Verbal Dyspraxia’. The American Journal of Human Genetics 79 (5): 965–72. https://doi.org/10.1086/508902.

French, C. A., X. Jin, T. G. Campbell, et al. 2012. ‘An Aetiological Foxp2 Mutation Causes Aberrant Striatal Activity and Alters Plasticity during Skill Learning’. Molecular Psychiatry 17 (11): 1077–85. https://doi.org/10.1038/mp.2011.105.

Fujita, Eriko, Yuko Tanabe, Akira Shiota, et al. 2008. ‘Ultrasonic Vocalization Impairment of Foxp2 (R552H) Knockin Mice Related to Speech-Language Disorder and Abnormality of Purkinje Cells’. Proceedings of the National Academy of Sciences of the United States of America 105 (8): 3117–22. https://doi.org/10.1073/pnas.0712298105.

Fujita-Jimbo, Eriko, Genri Kawahara, and Takashi Momoi. 2026. ‘Foxp2 Mutations and Abnormal Brain and Gastrointestinal Development: Insights from Animal Models of Speech-Language and Autism Spectrum Disorders’. *Frontiers in Neuroanatomy* 20 (March). https://doi.org/10.3389/fnana.2026.1783101.

Gordon, Jennifer, Shohreh Amini, and Martyn K. White. 2013. ‘General Overview of Neuronal Cell Culture’. In Neuronal Cell Culture: Methods and Protocols, edited by Shohreh Amini and Martyn K. White. Humana Press. https://doi.org/10.1007/978-1-62703-640-5_1.

Groot, Nikita E. 2026. ‘Talking Transgenics: Towards Establishing Transgenic Bats as a Mammalian Model of Vocal Learning’ PhD diss., University of St. Andrews

Hachigian, Lea J., Vitor Carmona, Robert J. Fenster, et al. 2017. ‘Control of Huntington’s Disease-Associated Phenotypes by the Striatum-Enriched Transcription Factor Foxp2’. *Cell Reports* 21 (10): 2688–95. https://doi.org/10.1016/j.celrep.2017.11.018.

Haesler, Sebastian, Christelle Rochefort, Benjamin Georgi, Pawel Licznerski, Pavel Osten, and Constance Scharff. 2007. ‘Incomplete and Inaccurate Vocal Imitation after Knockdown of FoxP2

in Songbird Basal Ganglia Nucleus Area X'. PLOS Biology 5 (12): e321. https://doi.org/10.1371/journal.pbio.0050321.

Hannenhalli, Sridhar, and Klaus H. Kaestner. 2009. 'The Evolution of Fox Genes and Their Role in Development and Disease'. Nature Reviews. Genetics 10 (4): 233–40. https://doi.org/10.1038/nrg2523.

Hoed, Joery den, Karthikeyan Devaraju, and Simon E. Fisher. 2021. 'Molecular Networks of the FOXP2 Transcription Factor in the Brain'. The EMBO Reports 22 (8): EMBR202152803. https://doi.org/10.15252/embr.202152803.

Hoed, Joery den, and Simon E. Fisher. 2020. 'Genetic Pathways Involved in Human Speech Disorders'. Current Opinion in Genetics & Development, Molecular and Genetic Bases of Disease, vol. 65 (December): 103–11. https://doi.org/10.1016/j.gde.2020.05.012.

Janik, Vincent M., and Mirjam Knörnschild. 2021. 'Vocal Production Learning in Mammals Revisited'. *Philosophical Transactions of the Royal Society of London. Series B, Biological Sciences* 376 (1836): 20200244. https://doi.org/10.1098/rstb.2020.0244.

Knörnschild, Mirjam, Martina Nagy, Markus Metz, Frieder Mayer, and Otto von Helversen. 2010. 'Complex Vocal Imitation during Ontogeny in a Bat'. Biology Letters 6 (2): 156–59. https://doi.org/10.1098/rsbl.2009.0685.

Lai, Cecilia S. L., Simon E. Fisher, Jane A. Hurst, Faraneh Vargha-Khadem, and Anthony P. Monaco. 2001. 'A Forkhead-Domain Gene Is Mutated in a Severe Speech and Language Disorder'. Nature 413 (6855): 519–23. https://doi.org/10.1038/35097076.

Lattenkamp, Ella Z., Sonja C. Vernes, and Lutz Wiegrebe. 2018. 'Volitional Control of Social Vocalisations and Vocal Usage Learning in Bats | Journal of Experimental Biology | The Company of Biologists'. The Company of Biologists. https://doi.org/10.1242/jeb.180729.

Lattenkamp, Ella Z., Sonja C. Vernes, and Lutz Wiegrebe. 2020. 'Vocal Production Learning in the Pale Spear-Nosed Bat, Phyllostomus Discolor'. Biology Letters 16 (4): 20190928. https://doi.org/10.1098/rsbl.2019.0928.

Li, Minghui, Yuhan Yuan, Zongkun Hou, Shilei Hao, Liang Jin, and Bochu Wang. 2024. 'Human Brain Organoid: Trends, Evolution, and Remaining Challenges'. Neural Regeneration Research 19 (11): 2387. https://doi.org/10.4103/1673-5374.390972.

Liu, Xiaofeng, Zhiyuan Zhou, Yao Zhang, Hao Zhong, Xiulei Cai, and Rongfa Guan. 2025. 'Recent Progress on the Organoids: Techniques, Advantages and Applications'. Biomedicine & Pharmacotherapy 185 (April): 117942. https://doi.org/10.1016/j.biopha.2025.117942.

MacDermot, Kay D., Elena Bonora, Nuala Sykes, et al. 2005. 'Identification of FOXP2 Truncation as a Novel Cause of Developmental Speech and Language Deficits'. American Journal of Human Genetics 76 (6): 1074–80. https://doi.org/10.1086/430841.

Merchán, Ana, Laura Fernández García, Nahuel Gioiosa Maurno, Pamela Ruiz Castañeda, and María Teresa Daza González. 2022. 'Executive Functions in Deaf and Hearing Children: The Mediating Role of Language Skills in Inhibitory Control'. Journal of Experimental Child Psychology 218 (June): 105374. https://doi.org/10.1016/j.jecp.2022.105374.

Murugan, Malavika, Stephen Harward, Constance Scharff, and Richard Mooney. n.d. 'Diminished FoxP2 Levels Affect Dopaminergic Modulation of Corticostriatal Signaling Important to Song Variability: Neuron'. Cell Press journal. Accessed 18 August 2026. https://www.cell.com/neuron/fulltext/S0896-6273(13)00852-0.

Patel, Rohankumar, and Ankur Patel. n.d. '(PDF) In Vivo-In Vitro Correlation (IVIVC) in Drug Development: Bridging Preclinical and Clinical Outcomes for Regulatory Approvals'. World Journal of Advanced Research and Reviews. https://doi.org/10.30574/wjarr.2024.22.2.1197.

Prat, Yosef, Mor Taub, and Yossi Yovel. 2015. 'Vocal Learning in a Social Mammal: Demonstrated by Isolation and Playback Experiments in Bats | Science Advances'. Science Advances. https://doi.org/10.1126/sciadv.1500019.

Reuter, Miriam S., Angelika Riess, Ute Moog, et al. 2017. 'FOXP2 Variants in 14 Individuals with Developmental Speech and Language Disorders Broaden the Mutational and Clinical Spectrum'. Phenotypes. Journal of Medical Genetics 54 (1): 64–72. https://doi.org/10.1136/jmedgenet-2016-104094.

Rhijn, Jon-Ruben van, Simon E. Fisher, Sonja C. Vernes, and Nael Nadif Kasri. 2018. 'Foxp2 Loss of Function Increases Striatal Direct Pathway Inhibition via Increased GABA Release'. Brain Structure and Function 223 (9): 4211–26. https://doi.org/10.1007/s00429-018-1746-6.

Schulz, S. B. 2010. 'Knockdown of FoxP2 Alters Spine Density in Area X of the Zebra Finch'. Wiley Online Library. https://onlinelibrary.wiley.com/doi/full/10.1111/j.1601-183X.2010.00607.x.

Sharma, Akshay. 2026. 'Gene Therapy for Sickle Cell Disease: Practice Recommendations from the American Society for Transplantation and Cellular Therapy and the International Society for Cell & Gene Therapy - Transplantation and Cellular Therapy, Official Publication of the American Society for Transplantation and Cellular Therapy'. American Society for Transplantation and Cellular Therapy. https://doi.org/10.1016/j.jtct.2026.03.019.

Suresh, Shravanti. 2021. 'Beginner's Guide to CRISPR-Cas9-Based Gene Editing'. The Biochemist 43 (4): 36–40. https://doi.org/10.1042/bio_2021_131.

Vernes, Sonja C., Paolo Devanna, Stephen Gareth Hörpel, et al. 2022. 'The Pale Spear-Nosed Bat: A Neuromolecular and Transgenic Model for Vocal Learning'. Annals of the New York Academy of Sciences 1517 (1): 125–42. https://doi.org/10.1111/nyas.14884.

Wang, Bin, Danjuan Lin, Chuan Li, and Philip Tucker. 2003. 'Multiple Domains Define the Expression and Regulatory Properties of Foxp1 Forkhead Transcriptional Repressors* - Journal of Biological Chemistry'. Journal of Biological Chemistry. https://doi.org/10.1074/jbc.M207174200.

Weigel, D., and H. Jäckle. 1990. 'The Fork Head Domain: A Novel DNA Binding Motif of Eukaryotic Transcription Factors?' Cell 63 (3): 455–56. https://doi.org/10.1016/0092-8674(90)90439-l.

Zhu, Xiaoquan, Chao Chen, Dong Wei, et al. 2023. 'FOXP2 Confers Oncogenic Effects in Prostate Cancer'. eLife 12 (September): e81258. https://doi.org/10.7554/eLife.81258.

Zou, Yixin, Wai Han Yiu, Sarah W. Y. Lok, et al. 2025. 'Tubular FoxP2 and Kidney Fibrosis : Journal of the American Society of Nephrology'. Journal of the American Society of Nephrology. https://doi.org/10.1681/ASN.0000000576.

6 APPENDICES

Appendix 1: Primer Optimisation

Table 3: primer optimisation plan. Central temperatures were decided per optimal library temperatures and were tested against two additional temperatures to either side (±2, ±4).

COLUMN	2	3	4	5	6	7	8	9	10	11
TEMP	61.8	62.8	64	65	66	67.1	68.2	69.2	70.3	71.1
Bat Guide 7 Pair 1										
Bat Guide 7 Pair 2										
Bat Guide 8 Pair 1										
Bat Guide 8 Pair 2										
Human Guide 7 Pair 1										
Human Guide 7 Pair 2										
Human Guide 8 Pair 1										
Human Guide 8 Pair 2										

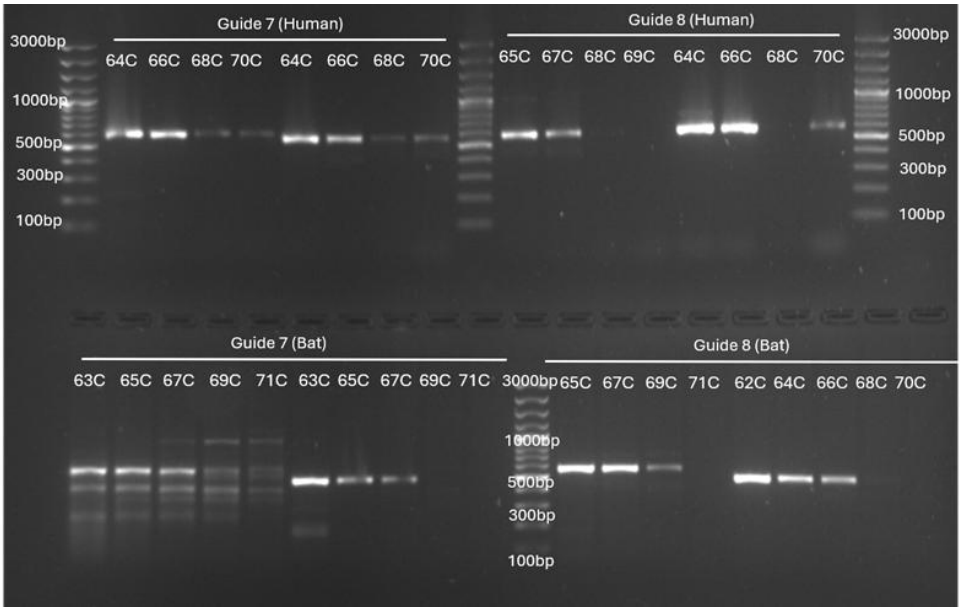

Fig 9: Efficiency of primers at different temperatures. Specificity denoted by single bands (present in all conditions with the exception of guide 7 pair 1 in bat DNA (red square, bottom left)). Strength of amplification measured by the intensity of bands. Favourable guide pairs are decided by degree of specificity. Favourable temperatures are decided by the strength of amplification.

Appendix 2: Checking PCR Amplification Specificity

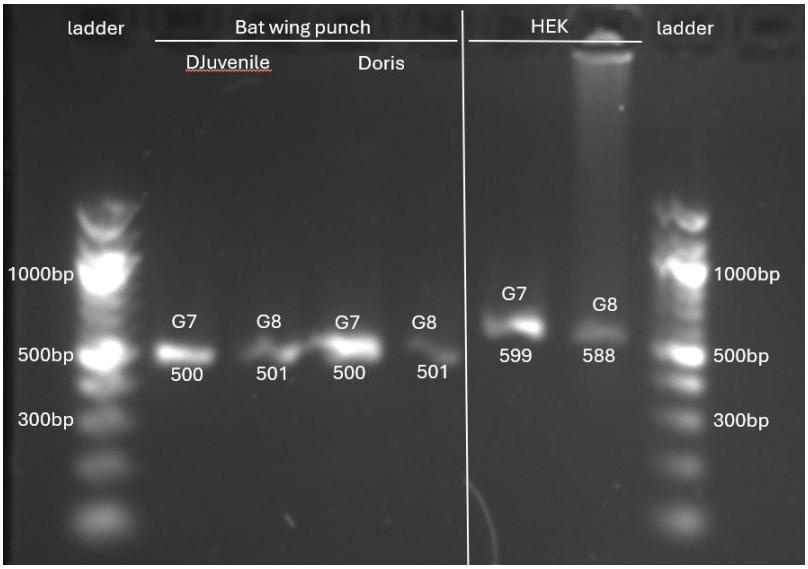

Fig 10: If amplification is specific, a fragment of a single size, decided by the given primer pair, is amplified. Specific amplification is observed in all conditions. HEK guide 8 exhibits smearing. Calculation of sample volume post-amplification shows greater volume of HEK guide 7 and HEK guide 8 amplicon samples than 46uL (the greatest possible volume if no loss of volume occurs, considering that 4uL were used to run the gel). Both HEK conditions are replicated to ensure integrity of PCR amplicons for ensuing DNA digest.

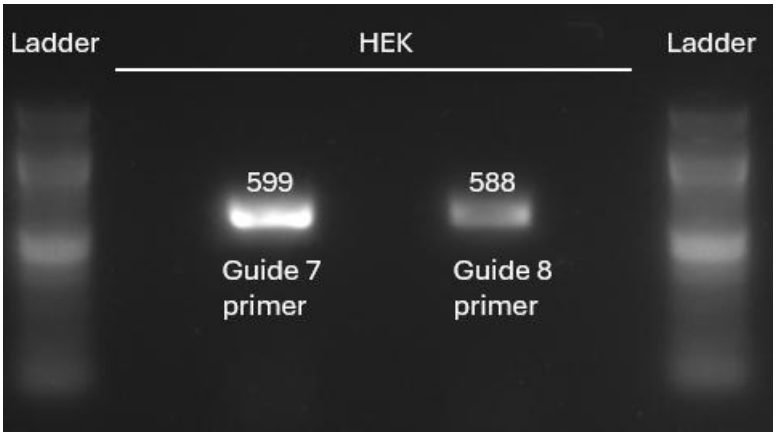

Fig 11: HEK conditions replicated. Exhibit specific amplification. No smearing present. Volumes of post-PCR, post-gel samples sit between 42 and 44uL.

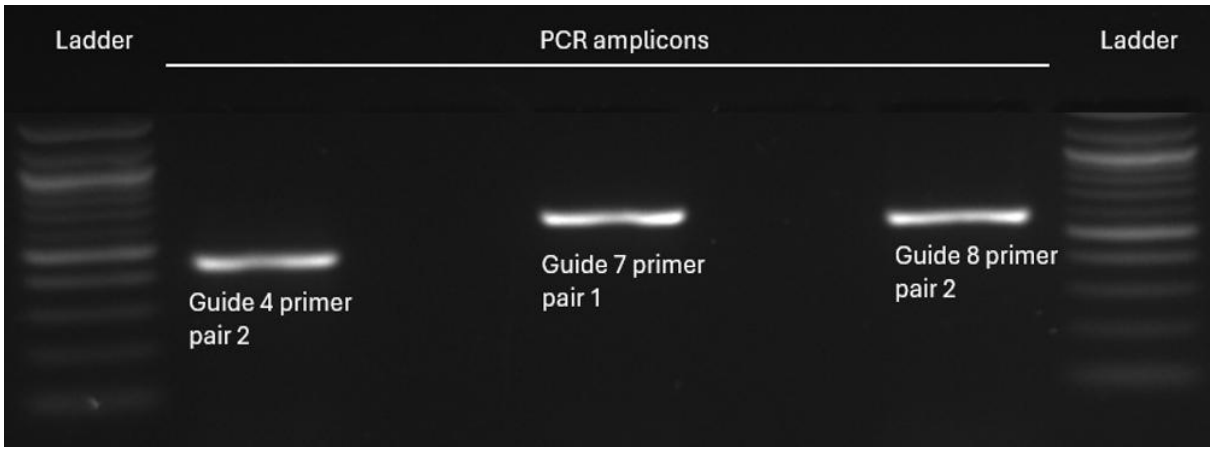

Fig 12: PCR amplification specificity check of PCR and DNA digest replication of HEK DNA following the unsuccessful cleavage of guide 8 HEK DNA. Includes positive control.

Appendix 3: Additional Gel Images Used For Measuring Cleavage Efficiency

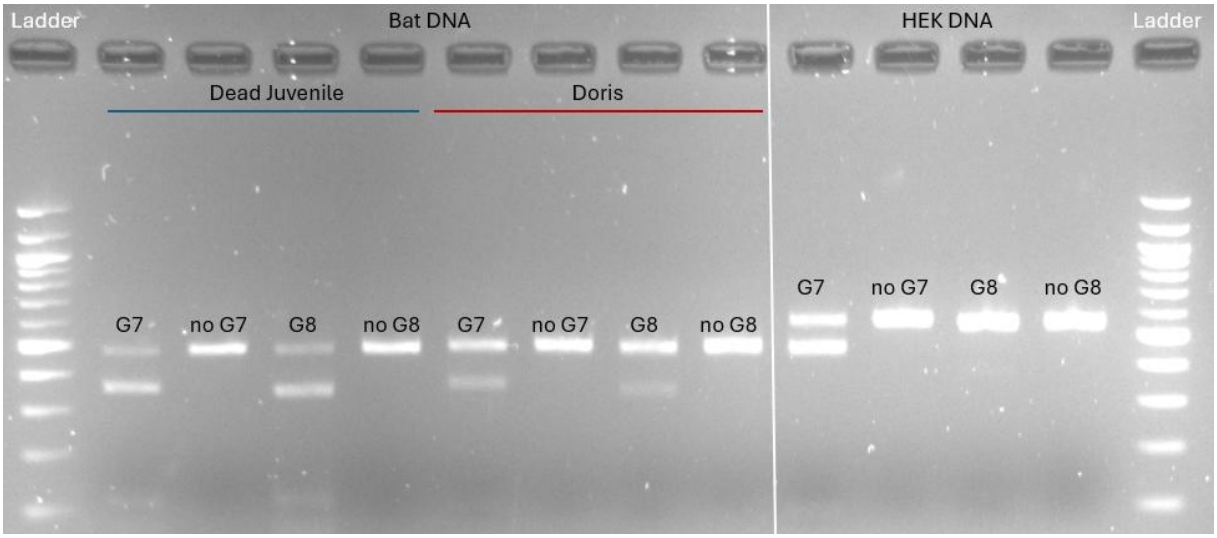

Fig 13: Overexposed version of gel seen in figure 6 (see *Fig 9* for gel explanation). Overexposing gels allows better measuring of cleavage efficiency when bands are faint.

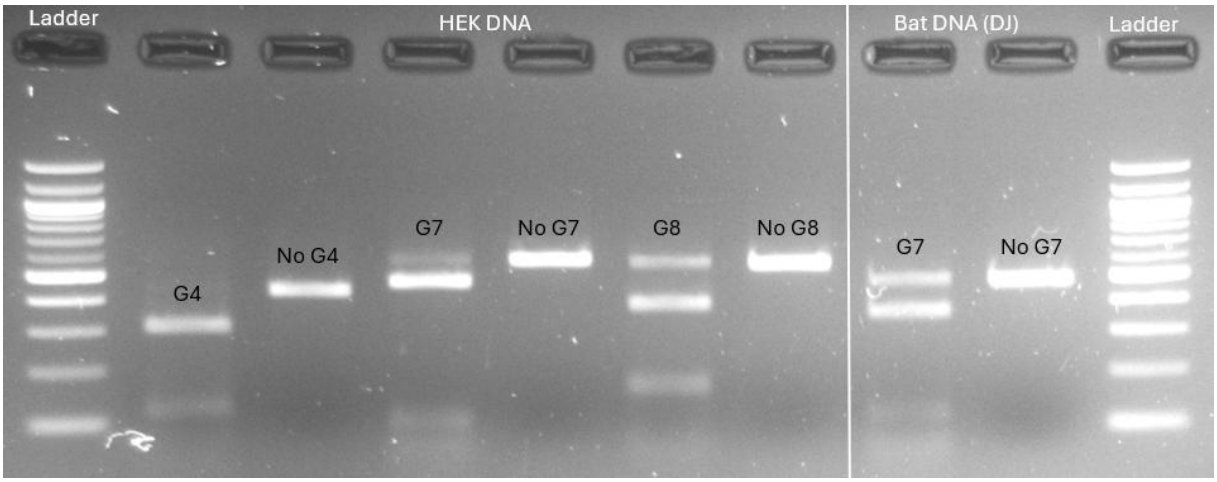

Fig 14: Overexposed version of gel seen in figure 7 (see *Fig 10* for gel explanation). Overexposing gels allows better measuring of cleavage efficiency when bands are faint.

Appendix 4: Calculated Cleavage Efficiency (Gel Analyzer 26.1)

Table 4: Cleavage Efficiency, Gels 1 (*Fig 9*) & 2 (*Fig 10*)

	Gel 1		**Gel 2**		
	guide 7 cleavage efficiency (%)	guide 8 cleavage efficiency (%)	guide 7 cleavage efficiency (%)	guide 8 cleavage efficiency (%)	guide 4 cleavage efficiency (%)
DJ	59.8	58.6	49.1		
Doris	23.9	15			
HEK	52.5		81.4	55.1	89.7